H-induced Restructuring on Cu(111) Triggers CO Electro-reduction in Acidic Electrolyte

Dongfang Cheng¹, Anastassia N Alexandrova^{2,3,4}*, Philippe Sautet^{1,2,4}*

¹Department of Chemical and Biomolecular Engineering, University of California, Los Angeles, CA 90095, USA.

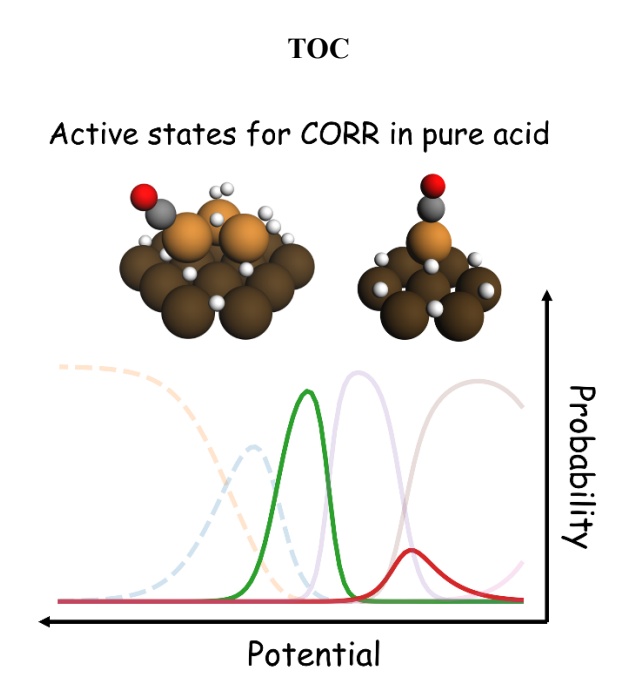
²Department of Chemistry and Biochemistry, University of California, Los Angeles, CA 90095, USA.

³Department of Materials Science and Engineering, University of California, Los Angeles, CA 90095, USA.

⁴California NanoSystems Institute, Los Angeles, CA 90095, USA.

^{*} Correspondence: ana@chem.ucla.edu, sautet@ucla.edu

Abstract: In acidic conditions, the electro-reduction of CO or CO₂ (noted CO₍₂₎RR) on metal surfaces is conventionally hindered by intense competition with the hydrogen evolution reaction (HER). In this study, we present first principle calculations of a mechanism wherein the formation of H-induced Cu adatoms on Cu(111) serves as a pivotal trigger for CORR in acidic environments. Through an analysis of the grand canonical surface state population, we elucidate that these newly formed adatoms create an array of active sites essential for both CO adsorption and subsequent reduction. Our ensemble-based kinetic models unveil the role of adatoms, enhancing HER while simultaneously initiating CORR. Notably, the cumulative activity of HER and CORR is contingent upon the combination of various surface states, with their individual contributions varying based on electrode potential and pH. The interplay between surface state dynamics and electrochemical activity sheds new light on the potential dependent nature of the active site and reaction kinetics governing CORR on Cu(111) in acidic media.



The electro-reduction of CO or CO₂ (CO₍₂₎RR) to valuable products on Cu surfaces holds promise as a pathway toward carbon neutrality¹⁻⁴. Despite its potential to suppress carbonate/bicarbonate formation and aid proton transfer, acidic CO₍₂₎RR is hindered by the active hydrogen evolution reaction (HER)⁵⁻⁸. Various strategies, including the introduction of alkaline cations⁹, have been explored to create local alkaline microenvironments to mitigate this challenge.

In acidic conditions, the exceptionally high concentration of protons facilitates their rapid adsorption onto electrode surfaces, making CO₂ or CO adsorption highly unfavorable partly due to active site blocking, which elucidates why CO₍₂₎RR is usually undetectable under acidic electrolytes without local microenvironment regulation^{7,9}. Intriguingly, an early work by Koper and coll. revealed the production of CH₄ from CORR on Cu(111) surfaces in pure acidic electrolytes without alkaline cations, suggesting the creation of novel active sites for CORR¹⁰. Our recent work demonstrated that under negative potential, Cu(111) undergoes restructuring upon high H coverage, from proton reduction, leading to the formation of low coordination Cu adatoms in acidic conditions¹¹. We hypothesize that these H adsorbate-induced Cu adatoms may provide potential opportunities for CORR to generate CH₄, as seen in experiments.

In this study, we demonstrate that in an acidic solution and under reducing conditions, the formation of H-induced adatoms on the Cu(111) surface initiates the CORR by introducing active sites for CO adsorption and reaction. Upon Cu restructuring, CO competes with protons for adsorption onto the adatoms, leading to subsequent reduction reactions. In contrast, these adatoms cannot stabilize CO₂ or two co-adsorbed CO, thereby impeding both CO₂RR and C₂ production from CORR, in line with experimental observations. We systematically investigate the electrode potential and pH-dependent grand canonical surface ensembles, encompassing varied densities of Cu adatoms or small clusters, as well as different coverages of *H and *CO in acidic conditions. Through an ensemble-based kinetic model, we elucidate that these restructured surface states not only enhance the HER but also create opportunities for CORR.

Under acidic electroreduction conditions, H will achieve high coverage from thermodynamic analysis (Figure S1) and experimental STM evidence^{11,12}. Consequently, non-restructured Cu(111) surfaces, covered with H, exhibit unfavorable binding for CO₂/CO molecules. This results in markedly low coverage of CO₂/CO species on the surface (Figure S2), thus impeding CO₍₂₎RR. Notably, our recent study showed that on Cu(111) surface, as the potential becomes more negative, strong H adsorption induces the formation of isolated Cu adatoms decorated with two nearly-associated H atoms (noted *H-H) in a (4*4) unit cell, followed by ad-clusters such as Cu trimers for even more negative potential. Such restructured surfaces readily undergo the Tafel step, leading to H₂ gas generation, while also facilitating proton exchange between adatoms and the surrounding solution, thereby enhancing the HER activity, as demonstrated in our prior research.

This intriguing observation piqued our interest: during the proton exchange process, can CO₂ or CO compete with protons to bind with the adatoms/ad-clusters in acidic conditions? If CO₂ or CO could bind

to the adatoms, they might undergo subsequent reduction. The first restructured termination under reducing potential observed from experiment and theory (noted A1-15) contains one Cu adatom with 15H in a (4*4) unit cell^[5]. We show here that, on this structure, one CO molecule can compete with hydrogen adsorbates within a specific potential range, exhibiting a similar energy compared to the adsorption of the two H atoms (*H-H) adsorption (Figure S3).

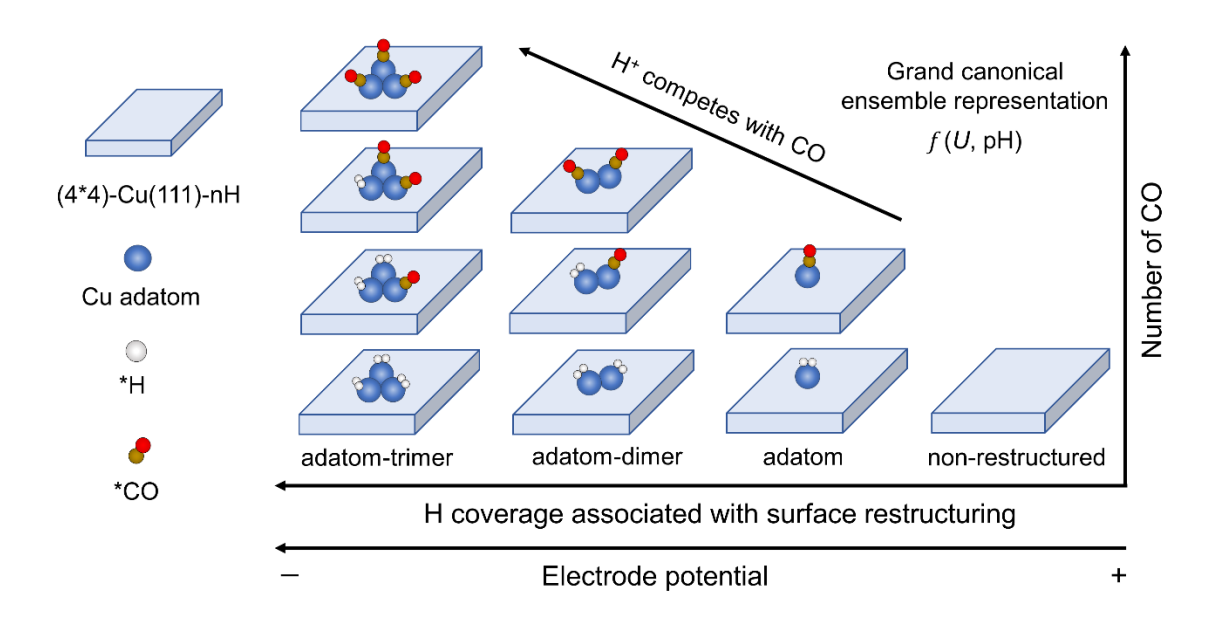


Figure 1. Schematic representation of the H-induced restructuring of Cu(111) in reducing conditions by adatom/ad-cluster formation and how it may trigger CO adsorption and CORR in acidic conditions. On the Cu adatoms *H represents adsorbed H atoms from proton reduction (which appear as nearly-associated pairs) and *CO represents CO adsorption.

Motivated by the comparable adsorption energy of CO relative to *H-H, we systematically replace *H-H with CO on the Cu adatom and on Cu ad-clusters that form at more negative potential within the ensemble of H-covered Cu(111) surfaces, which comprised non-restructured surfaces as reference (NR), surfaces featuring adatoms (A1), adatom-dimer configurations (A2), and adatom-trimer arrangements (A3). This systematic substitution yields a new structure ensemble characterized by diverse adatom densities and *CO and *H coverages. Subsequently, grand canonical density functional theory (GCDFT) calculations are employed to obtain the potential- and pH-dependent grand canonical ensemble representation, which provides a detailed picture of the dynamic surface states across the reaction potential range and solution pH (Figure 1 and Figure S4).

We use Boltzmann statistics at room temperature (298.15 K) to approximate the population distribution of all surface states within the complex ensemble to understand the structural evolution as the function of

potential and pH. It allows us to consider not only the global minima (GM) of the surface at each potential but also the metastable structures (MS), since it was shown that the latter can be the main contributor to the catalytic activity in some cases¹³⁻¹⁷. This approach assumes that surface restructuring is fast with respect to experimental reaction time scale. One can underline that in the experiments of Koper and coll.¹⁰ the potential scan was slow (1 mV/s) which leaves significant time for the atomic diffusion process required to form the adatoms/ad clusters under potential. However, calculating the kinetics of the restructuring is very challenging and is not addressed here, so that the equilibrium between surface structures remains a hypothesis, only validated a posteriori by comparing the catalytic activity with experiment.

Under weakly negative potentials (-0.3 V), the surface is predominantly covered with a high density of H atoms without undergoing restructuring (NR-11 and NR-12 with 11 and 12 H atoms in the 4×4 unit cell respectively.). Upon reaching a threshold potential (~-0.45 V at pH=1), H adsorbates induce the formation of one adatom (A1-15) with one H₂ molecule adsorbed per adatom in a (4*4) unit cell. During the fast exchange of protons between adatom and solution, CO competes with protons, leading to the formation of A1-13-CO, where one CO molecule is adsorbed per adatom, replacing the *H-H unit. A1-13-CO represents a minor fraction of the ensemble within a narrow potential range (20% at -0.48 V vs SHE). Subsequently, at even more negative potential, the A3 Cu ad-trimer structures becomes more stable and probable. It could be formed by the aggregation of adatoms¹⁸ or the extraction of three atoms from the steps¹⁹. Notably, one specific ad-trimer configuration featuring one CO adsorption on one of the adatoms, together with one *H-H on each of the other Cu atoms of the trimer (A3-19-CO) is remarkably stable at around -0.6 V vs. SHE. Although the Cu ad-trimer could in principle chemisorb two or three CO, the competition with hydrogen adsorption at potential for which the ad-trimer is stable is not very favorable, so that these structures with multiple COs show negligible probabilities. For the probability of each surface state and different pH conditions, see Figure S5-S7.

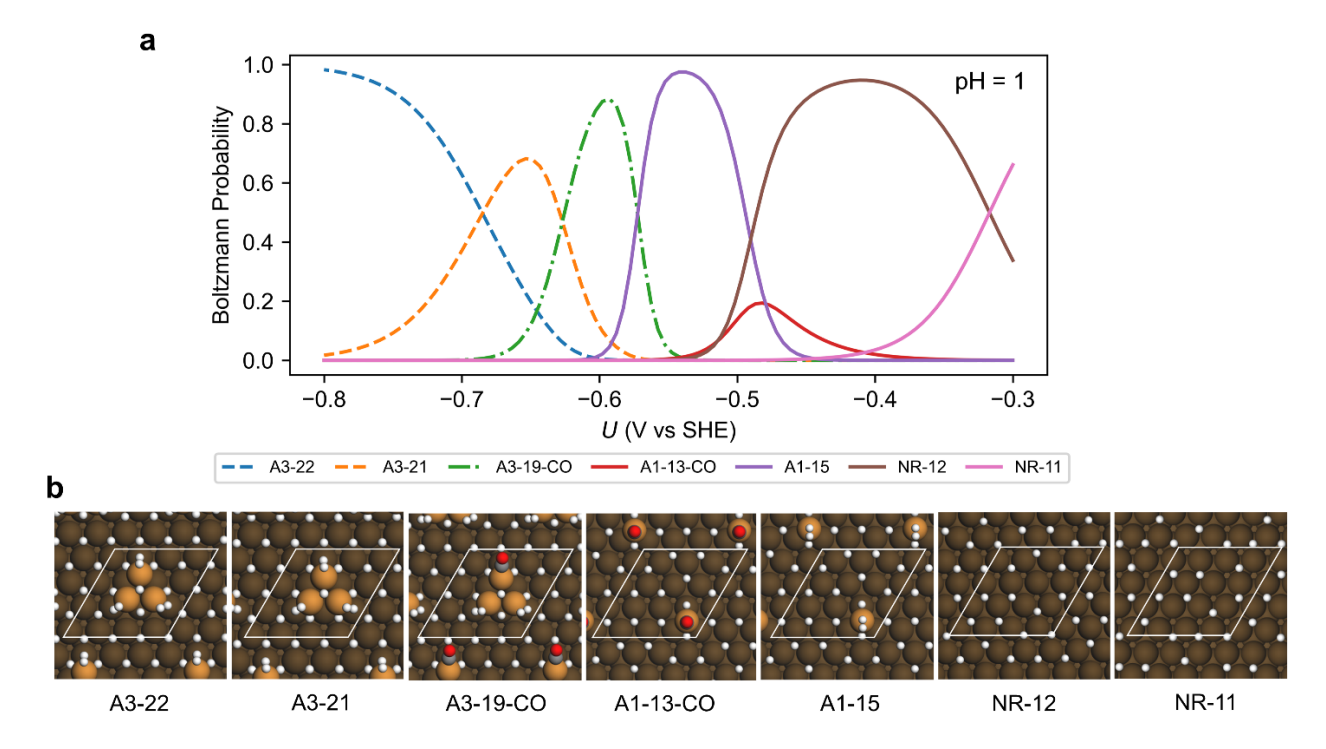


Figure 2. The ensemble representation of Cu(111) at pH=1. (a) Boltzmann probability of each surface state as the function of electrode potential versus SHE (surfaces with probability less than 0.1% are not shown in the figure). NR-X indicates the non-restructured Cu(111) surface with X H adsorbates in the (4*4) unit cell, while An-X indicates the formation on the surface of an Cu adatom (n=1) or a Cu trimer (n=3) with X H atom. An additional CO in the name just underlines the presence of a CO adsorbate. (b) The atomic structures of the surface which are shown in the probability diagram. The room temperature, 298.15 K, is adopted in this work. Color code: dark brown: surface Cu, light brown: adatom, white: H, grey: C, red: O.

Upon reaching more negative potentials, proton adsorption becomes even more favorable, and no structures with CO adsorption are observed. The probability diagram derived from the whole ensemble indicates that the restructuring induced by H offers the opportunity for CO adsorption. Among the various ensembles studied, two specific surface states, namely A1-13-CO and A3-19-CO, exhibit relatively higher stability within specific potential ranges. These states hold the potential to facilitate CO reduction owing to their relatively stable configurations and CO adsorption capabilities. However, these restructured Cu surfaces cannot favorably bind CO₂ or two CO molecules in competition with hydrogen adsorption across the entire potential range of interest, in line with the absence of CO₂RR activity and the lack of C₂ product generation from CORR in experiments. Note that our sampling stops at the A3 state, suggesting the possibility of other surface states at even more negative potentials, which are not considered in this work since CO would not be able to compete with hydrogen at these potentials.

We then present the CORR reaction pathways on three representative surfaces, NR-12, A1-13-CO, and A3-19-CO (Figure 3a). We observe that CO adsorption on non-restructured surfaces, subject to a high hydrogen coverage at the considered potential, is energetically unfavorable (Figure 3b), resulting in a very low CO coverage (~10⁻⁶ ML) on NR surfaces (Figure 3c). In contrast, CO adsorption on adatom and adatom-trimer

structures featuring ultra-low coordination numbers, is considerably stronger, allowing for near-complete coverage on adatoms in the absence of H adsorption. Our calculations show that *CO protonation to *CHO is the rate-determining step across all the surfaces, in agreement with previous studies on non-restructured Cu(111)^{20, 21}. We observe lower energy barriers for this crucial step on adatoms/ad-clusters compared to NR surfaces (Figure 3b), highlighting that the conversion of CO to *CHO has a favorable kinetics on adatoms. The elementary steps after forming *CHO are all exothermic, and we assume that there are no additional significant barriers after that. The other possible reaction pathways are shown in Figure S8. It should be noted that the surface coverage of H remains constant throughout the reaction coordinates. Scenarios involving surface-bound H participating in the hydrogenation reaction are not favorable due to the higher calculated barrier compared to cases where the proton source is H⁺ from the solution stabilized with water clusters (Figure S9).

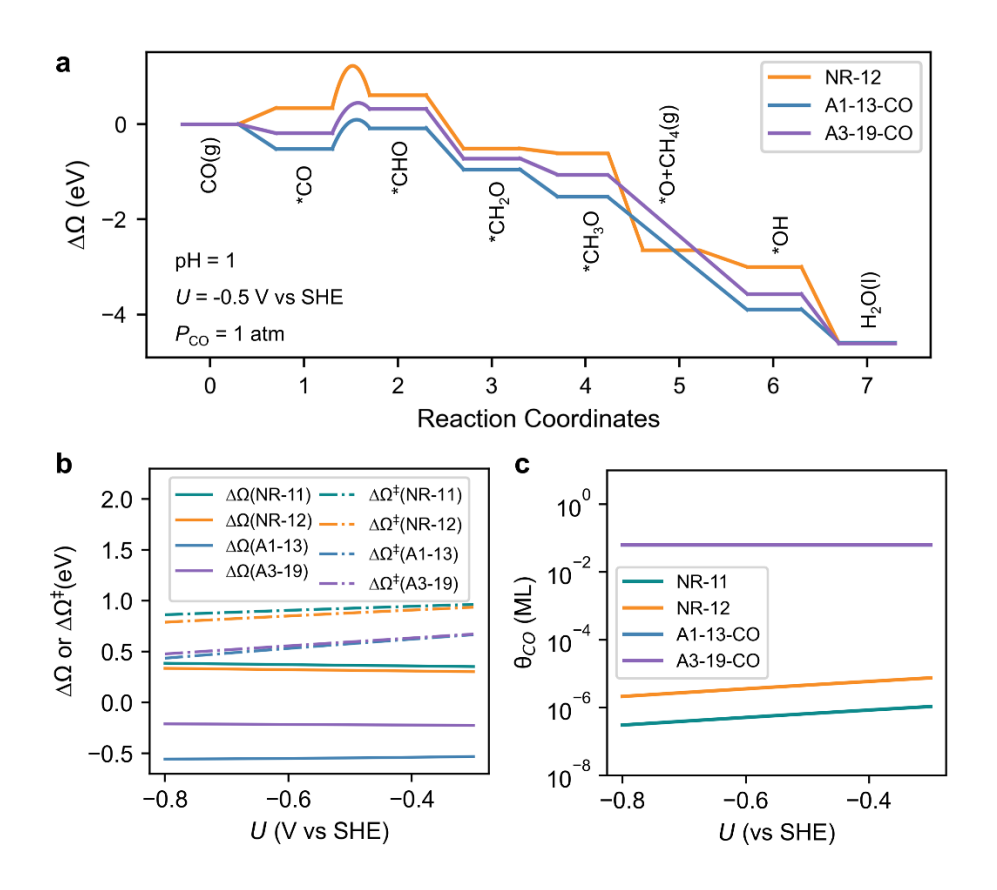


Figure 3. CORR pathway shows a more favorable energy profile on restructured Cu surfaces in acidic conditions. (a) Gibbs free energy diagram of CORR on NR-12, A1-13-CO and A3-19-CO surfaces under -0.5 V vs SHE and pH 1. For A1-13-CO and A3-19-CO, *O will quickly be protonated to *OH, thus the energies of *O are not shown in the figure. (b) Reaction energy ($\Delta\Omega$) for CO adsorption and reaction barrier ($\Delta\Omega^{\ddagger}$) for *CO protonation to *CHO as the function of electrode potential. (c) CO coverage as the function of potential on representative surfaces based on the Langmuir adsorption model. Note that A1-13-CO is not visible in the figure due to the overlap with A3-19-CO.

Based on the energy profiles, we conducted ensemble-based activity analysis for both HER and CORR. In the case of HER, our prior study¹¹ and kinetic calculations (Figure S10) reveal that the reaction on the surface with adatoms is limited by the Volmer step. Conversely, on the non-restructured surfaces, the Heyrovsky step is identified as the rate-determining step. Our simulated current density, illustrated in Figure 4a, unequivocally demonstrates that surfaces hosting adatoms significantly enhance the HER activity. Considering both surface population and individual activity, we found that the total current density is initially determined by the NR surfaces. However, once the adatom forms (at ~-0.45 V vs SHE), a sudden enhancement in current density occurs. This enhancement is predominantly contributed by the presence of adatoms and subsequently of the ad-trimer structures, as depicted in Figure 4b. This observation reaffirms adatoms/ad-clusters as the predominant active sites for HER activity on the Cu(111) surface under acidic conditions.

In the context of CORR, our analysis focuses on the comparison of CORR activity between non-restructured Cu(111) terrace sites (NR-11 and NR-12) and the restructured adatom sites (A1-13-CO, and A3-19-CO). The other high H coverage surfaces are not considered given that the active sites are all blocked, and CO coverage should be extremely low. As depicted in Figure 4c and 4d, non-restructured surfaces exhibit negligible activity throughout the entire potential range. In contrast, surfaces with adatoms demonstrate the ability to initiate CORR. The onset potential for CORR activity is slightly delayed compared to HER, owing to the limited occurrence of A1-13-CO and A3-19-CO configurations and the insurmountable barriers associated with *CO protonation at relatively positive potentials. Specifically, A1-13-CO primarily contributes to the overall activity in the less negative potential region (around -0.58 V vs SHE), while A3-19-CO becomes significant in the more negative potential zone (around -0.68 V vs SHE). The observed valley between the two negative peaks arises from the limited populations of A1-13-CO and A3-19-CO states in that specific region.

A striking contrast is observed in Figure 4e. Compared to the non-restructured surfaces which show no CORR activity, reconstructed surfaces, formed by the presence of adatoms, trigger the CORR, leading to an increase in activity by several orders of magnitude. Such phenomenon can be attributed to two factors, namely CO coverage and CO hydrogenation barriers. The unfavorable CO adsorption on non-restructured surfaces not only results in extremely low CO coverage but also implies a significantly higher effective barrier, encompassing both CO adsorption energy and hydrogenation barrier. Moreover, as the pH decreases, we observed a shift of the onset potential of COR towards more positive potential and an increase in activity due to the increased concentration of protons. Regarding selectivity, it is evident that on non-restructured surfaces, HER exhibits 100% selectivity under acidic conditions. On reconstructed surfaces, while HER still dominates, there is a noticeable yield for CORR, indicating a shift in selectivity towards CORR. This observation highlights the phenomenon of self-activation exhibited by the Cu(111) surface under acidic conditions. The *H intermediate induces at high coverage the formation of adatoms, and such adatoms enable the surface to initiate CORR, altering the selectivity of the catalytic process. It should be noted that

our sampling of surface structures terminates at the ad-trimer, as our focus is primarily on the initial stage of CORR. However, it is possible that larger clusters, featuring CO adsorption, exist at more negative potentials, which potentially could contribute to the CORR activity, although adsorption competition with hydrogen would be unfavorable. Further work could extend to exploring a more comprehensive ensemble space across a broader range of potentials.

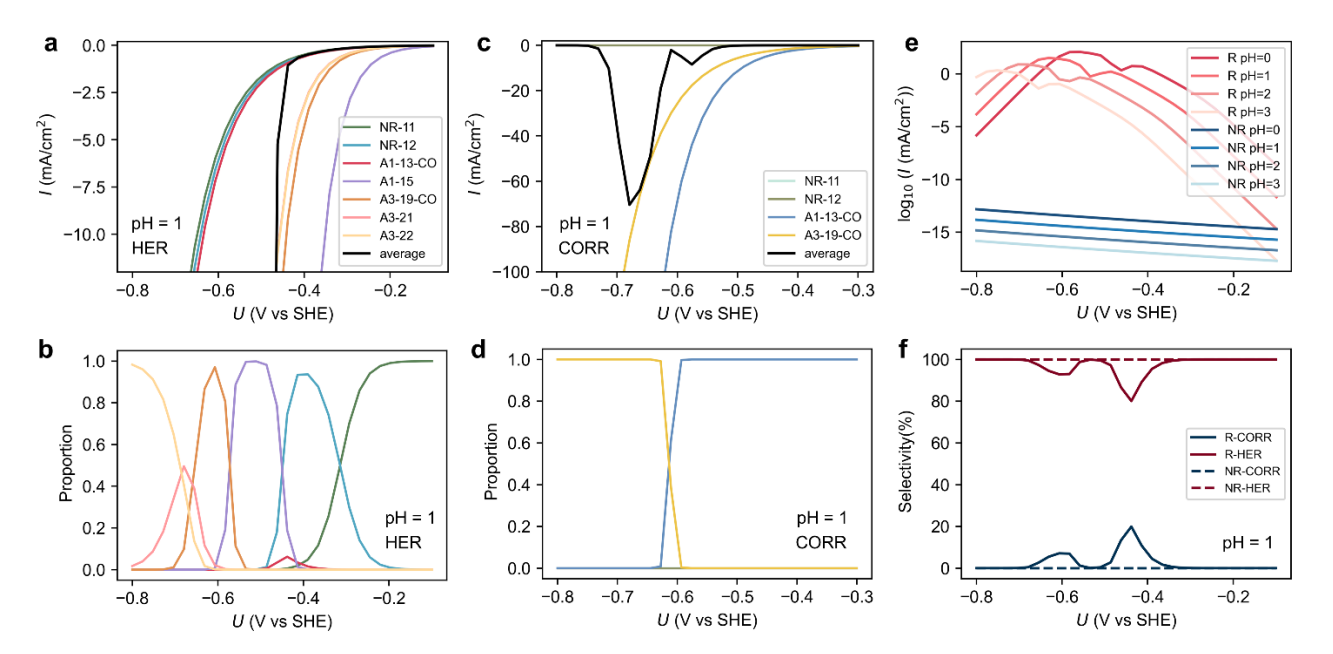


Figure 4. HER and CORR activity analysis. (a) For HER at pH=1, simulated current density of different surface structures and average current density considering the contributions of all the surface structures weighted by their Boltzmann probability at the considered potential. (b) Relative contribution of each surface structure for the HER activity as the function of potential. (c) For CORR at pH=1, simulated current density of different surface states and total current density considering the contributions of all the surface states. (d) CORR activity contribution of each surface state as the function of potential. (e) Comparison of CORR activity between reconstructed surfaces (R) and non-reconstructed surfaces (NR) at different pH conditions as a function of the potential. (f) Comparison of selectivity for HER and CORR between reconstructed and non-reconstructed surfaces at pH=1.

In summary, our study reveals the mechanism underlying acidic CORR on the Cu(111) surface. We demonstrate that, under potential, strong binding and high coverage of H induces the formation of Cu adatoms, providing new active sites for CO adsorption and subsequent reduction. Conversely, on non-reconstructed surfaces, CO adsorption is highly unfavorable due to the active site blocking caused by H adsorption. The electrode potential and pH-dependent grand canonical surface state population unveils the complex nature of Cu(111) surface in an acidic environment. This surface represents an ensemble characterized by varying densities of Cu adatoms and coverages of *H and *CO species. The ensemble-based kinetics model shows that the newly formed adatoms act as dual active sites, simultaneously facilitating both HER and CORR. The overall activities arise from a combination of various surface

structures. This work deciphers the active site for CORR under pure acidic conditions and introduces a non-static mechanism elucidating the self-activation of the Cu(111) surface towards CORR. Moreover, it highlights the two-way dynamic interplay between surface structures and electrochemical activity.

Further optimizing the $CO_{(2)}RR$ versus HER in acidic conditions requires the simultaneous suppression of H adsorption and enhancement of $CO_{(2)}$ adsorption. Several potential approaches can be proposed as a qualitative perspective. Firstly, one can refine the geometric configuration of active sites either by engineering ultra-low-coordinated sites on the catalyst surface or by employing single-atom catalysts. Such catalysts, characterized by narrower d-states and an elevated d-state average energy relative to terrace metal atoms, are anticipated to promote $CO_{(2)}$ adsorption more effectively. Secondly, we can manipulate the interfacial electric field, for example by introduction of alkaline cations, to leverage the large difference of dipole moments of adsorbed H and CO_2 . This adjustment can alter the field-dipole interaction, thereby modulating the relative adsorption energies of H and CO_2 . In addition, the introduction of partially positively charged sites, like heteroatom doping, can be beneficial for CO adsorption while the Volmer step can be suppressed due to the repulsive interplay between the positively charged active sites and protons. However, modulating only one such factor in isolation is hardly possible, as modifications of surface composition or electrolyte are likely to trigger different surface restructuring, changing also the types of available sites.

Supporting Information

The Supporting Information is available free of charge at https://pubs.acs.org/doi/XXXX. Method section, adsorption information of each adsorbate, Boltzmann probability analysis at different pH conditions, limitation of Boltzmann Statistics and the sensitivity of the calculated energetics on the DFT exchange-correlation functional and on the implicit solvent model.

Reference

- 1. Nitopi, S.; Bertheussen, E.; Scott, S. B.; Liu, X.; Engstfeld, A. K.; Horch, S.; Seger, B.; Stephens, I. E. L.; Chan, K.; Hahn, C.; Norskov, J. K.; Jaramillo, T. F.; Chorkendorff, I., Progress and Perspectives of Electrochemical CO₂ Reduction on Copper in Aqueous Electrolyte. *Chem. Rev.* **2019**, *119* (12), 7610-7672.
- 2. Dinh, C.-T.; Burdyny, T.; Kibria, M. G.; Seifitokaldani, A.; Gabardo, C. M.; García de Arquer, F. P.; Kiani, A.; Edwards, J. P.; De Luna, P.; Bushuyev, O. S.; Zou, C.; Quintero-Bermudez, R.; Pang, Y.; Sinton, D.; Sargent, E. H., CO₂ electroreduction to ethylene via hydroxide-mediated copper catalysis at an abrupt interface. *Science* **2018**, *360* (6390), 783-787.
- 3. Cheng, D.; Zhao, Z. J.; Zhang, G.; Yang, P.; Li, L.; Gao, H.; Liu, S.; Chang, X.; Chen, S.; Wang, T.; Ozin, G. A.; Liu, Z.; Gong, J., The nature of active sites for carbon dioxide electroreduction over oxide-derived copper catalysts. *Nat. Commun.* **2021**, *12* (1), 395.
- 4. Cheng, D.; Zhang, G.; Li, L.; Shi, X.; Zhen, S.; Zhao, Z. J.; Gong, J., Guiding catalytic CO₍₂₎ reduction to ethanol with copper grain boundaries. *Chem. Sci.* **2023**, *14* (29), 7966-7972.

- 5. Bondue, C. J.; Graf, M.; Goyal, A.; Koper, M. T. M., Suppression of Hydrogen Evolution in Acidic Electrolytes by Electrochemical CO₍₂₎ Reduction. *J. Am. Chem. Soc.* **2021**, *143* (1), 279-285.
- 6. Monteiro, M. C. O.; Philips, M. F.; Schouten, K. J. P.; Koper, M. T. M., Efficiency and selectivity of CO₍₂₎ reduction to CO on gold gas diffusion electrodes in acidic media. *Nat. Commun.* **2021**, *12* (1), 4943.
- 7. Xie, Y.; Ou, P.; Wang, X.; Xu, Z.; Li, Y. C.; Wang, Z.; Huang, J. E.; Wicks, J.; McCallum, C.; Wang, N.; Wang, Y.; Chen, T.; Lo, B. T. W.; Sinton, D.; Yu, J. C.; Wang, Y.; Sargent, E. H., High carbon utilization in CO₂ reduction to multi-carbon products in acidic media. *Nat. Catal.* **2022**, *5* (6), 564-570.
- 8. Zhao, Y.; Hao, L.; Ozden, A.; Liu, S.; Miao, R. K.; Ou, P.; Alkayyali, T.; Zhang, S.; Ning, J.; Liang, Y.; Xu, Y.; Fan, M.; Chen, Y.; Huang, J. E.; Xie, K.; Zhang, J.; O'Brien, C. P.; Li, F.; Sargent, E. H.; Sinton, D., Conversion of CO₂ to multicarbon products in strong acid by controlling the catalyst microenvironment. *Nat. Synth.* **2023**, *2* (5), 403-412.
- 9. Gu, J.; Liu, S.; Ni, W.; Ren, W.; Haussener, S.; Hu, X., Modulating electric field distribution by alkali cations for CO₂ electroreduction in strongly acidic medium. *Nat. Catal.* **2022**, *5* (4), 268-276.
- 10. Schouten, K. J. P.; Pérez Gallent, E.; Koper, M. T. M., The influence of pH on the reduction of CO and CO₂ to hydrocarbons on copper electrodes. *J. Electroanal. Chem.* **2014**, *716*, 53-57.
- 11. Cheng, D.; Wei, Z.; Zhang, Z.; Broekmann, P.; Alexandrova, A. N.; Sautet, P., Restructuring and Activation of Cu(111) under Electrocatalytic Reduction Conditions. *Angew. Chem. Int. Ed.* **2023**, *62* (20), e202218575.
- 12. Zhang, Z.; Wei, Z.; Sautet, P.; Alexandrova, A. N., Hydrogen-Induced Restructuring of a Cu(100) Electrode in Electroreduction Conditions. *J. Am. Chem. Soc.* **2022**, *144* (42), 19284-19293.
- 13. Sun, G.; Sautet, P., Metastable Structures in Cluster Catalysis from First-Principles: Structural Ensemble in Reaction Conditions and Metastability Triggered Reactivity. *J. Am. Chem. Soc.* **2018**, *140* (8), 2812-2820.
- 14. Sun, G.; Sautet, P., Active Site Fluxional Restructuring as a New Paradigm in Triggering Reaction Activity for Nanocluster Catalysis. *Acc. Chem. Res.* **2021**, *54* (20), 3841-3849.
- 15. Zhang, Z.; Zandkarimi, B.; Alexandrova, A. N., Ensembles of Metastable States Govern Heterogeneous Catalysis on Dynamic Interfaces. *Acc. Chem. Res.* **2020**, *53* (2), 447-458.
- 16. Baxter, E. T.; Ha, M.-A.; Cass, A. C.; Alexandrova, A. N.; Anderson, S. L., Ethylene Dehydrogenation on Pt_{4,7,8} Clusters on Al₂O₃: Strong Cluster Size Dependence Linked to Preferred Catalyst Morphologies. *ACS Catal.* **2017**, *7* (5), 3322-3335.
- 17. Ha, M. A.; Baxter, E. T.; Cass, A. C.; Anderson, S. L.; Alexandrova, A. N., Boron Switch for Selectivity of Catalytic Dehydrogenation on Size-Selected Pt Clusters on Al₍₂₎O₍₃₎. *J. Am. Chem. Soc.* **2017**, *139* (33), 11568-11575.
- 18. Amirbeigiarab, R.; Tian, J.; Herzog, A.; Qiu, C. R.; Bergmann, A.; Cuenya, B. R.; Magnussen, O. M., Atomic-scale surface restructuring of copper electrodes under CO electroreduction conditions. *Nat. Catal.* **2023**, *6*, 837-846
- 19. Sumaria, V.; Nguyen, L.; Tao, F. F.; Sautet, P., Atomic-Scale Mechanism of Platinum Catalyst Restructuring under a Pressure of Reactant Gas. *J. Am. Chem. Soc.* **2023**, *145* (1), 392-401.
- 20. Liu, X.; Xiao, J.; Peng, H.; Hong, X.; Chan, K.; Norskov, J. K., Understanding trends in electrochemical carbon dioxide reduction rates. *Nat. Commun.* **2017**, *8*, 15438.
- 21. Gauthier, J. A.; Lin, Z.; Head-Gordon, M.; Bell, A. T., Pathways for the Formation of C₂₊ Products under Alkaline Conditions during the Electrochemical Reduction of CO₂. *ACS Energy Lett.* **2022**, *7*(5), 1679-1686.

Acknowledgements

The work was supported by the National Science Foundation CBET grant 2103116 and the Audi CO₂ Cy Pres Award. Computational resources for this work were provided by the UCLA-shared cluster Hoffman2, the Innovative and Novel Computational Impact on Theory and Experiment (INCITE) program at the Argonne Leadership Computing Facility, which is a DOE Office of Science User Facility supported under Contract DE-AC02-06CH11357 and the Expanse cluster through the allocation CHE170060 at the San Diego Supercomputing Center through ACCESS. We thank Prof. Marc T. M. Koper for the fruitful discussion.

Data Availability

The data that support the findings of this study are available from the corresponding author upon reasonable request.

Conflict of Interest

The authors declare no conflict of interest.